Chemical Engineering Journal 318 (2017): 153-160

DOI: http://dx.doi.org/10.1016/j.cej.2016.06.029

CWPO of bisphenol A with iron catalysts supported on microporous carbons from grape seeds activation

Ismael F. Mena, Elena Diaz, Juan J. Rodriguez, Angel F. Mohedano[*].

Sección de Ingeniería Química, Facultad de Ciencias, Universidad Autónoma de Madrid, Campus de Cantoblanco, 28049 Madrid, Spain

[*]Corresponding author: Tel.: +34 914972680; Fax: +34 914973516

E-mail address: angelf.mohedano@uam.es

Abstract

The catalytic wet peroxide oxidation (CWPO) of bisphenol A (BPA) with Fe catalysts supported on activated carbon from grape seeds (GS) has been studied. The GS were pyrolized (N_2, 600 ºC, 2 h) and subjected to activation upon partial gasification with air (400 ºC, 2 h). Oxidized samples of the char and activated carbon were also obtained upon treatment with HNO_3. The Fe catalysts were prepared by incipient wetness impregnation with ferric nitrate solution. They showed narrow microporosity, with surface area values ≈ 350-500 m^2 g^{-1} and total iron contents between 2.8-4.2 % wt. The CWPO experiments were carried out at 50-80 ºC. The best catalyst allowed complete conversion of BPA (100 mg L^{-1}) and a 60 % TOC reduction in 3 h reaction time at 80 ºC and the theoretical stoichiometric amount of H_2O_2 (530 mg L^{-1}). The ecotoxicity of the effluent was negligible and the biodegradability was highly improved. In a long-term experiment (100 h), the catalyst suffered a loss of activity upon the early stages on stream (≈15 h), where about 20% of Fe was lost, followed by a highly stable behavior for the rest of the experiment.

Keywords: Grape Seeds, Heterogeneous Fenton, Bisphenol A, Fe catalysts, Biochar, Stability.

1. Introduction

One of the greatest challenges facing today's society is the correct management of the large amount of wastes produced. Agricultural wastes represent potential resources since they are available at low cost in their occurrence areas. Depending on the starting material, the pyrolysis of these wastes provides chars with certain characteristics of composition, porosity, specific surface area, pore structure and physicochemical properties [1,2]. Different kind of wastes have been studied to obtain char, like apricot and cherry stones [3], olive and grape bagasse [4] or pomegranate seeds [5]. Grape seeds represent up to 15% of the solid wastes from the wine industry [2]. The use of grape seeds for the preparation of adsorbents or catalytic supports appears very interesting owing to their granular morphology and their ready availability from winery works [2,6,7]. Satisfactory results have been obtained when this material has been used as adsorbent for the removal of diuron [7] or support of Pd catalyst in the hydrodechlorination of diuron [8] and in nitrate reduction [9].

Advanced oxidation processes (AOPs) have the capability to remove refractory or non-biodegradable pollutants operating at mild conditions [10,11]. Specifically, the potential of catalytic wet peroxide oxidation (CWPO), which implies the generation of HO· radicals from H_2O_2 decomposition has been widely investigated for the abatement of toxic and bio-recalcitrant organic pollutants in water [12-17]. Regarding the operating conditions, CWPO reactions are usually carried out at ambient-like conditions [18-20], but recent studies have reported significant improvement of the degradation and mineralization rates of recalcitrant compounds at temperatures above 50 ºC [13,15]. Inchaurrondo et al. [13] achieved 4-fold higher TOC conversion (from 20 to 80 %) in the CWPO of phenol by increasing the temperature from 25 to 70 ºC. The main drawbacks of CWPO is associated with the high requirements of H_2O_2. For this reason, many works focused on the amount of reactant needed as a main issue [14,15,21]. Traditionally CWPO Fe supported catalysts consist of silica, alumina, pillared clays and carbonaceous materials. The use of carbon materials as supports leads to highly dispersed metal

catalysts but they show relatively high iron leaching due to the acidic pH or the low chemical stability of the supports [14,22].

Bisphenol A (2,2-bis(4-hydroxyphenyl)propane, BPA) is an industrial chemical which is extensively consumed for polycarbonates manufacture as well as in the production of epoxy resins. Other applications include the manufacture of flame retardants such as tetrabromobisphenol A [23-25]. The world rate of production of this chemical (BPA) reached about 5.4 million tons in 2015 [26]. BPA is identified as an endocrine disrupting chemical, and it can be found in the water bodies either directly or indirectly via degradation of various BPA containing materials such as plastic bottles, containers, toys, food/soft drink cans, packaged food, etc. [27-29]. Because of its slow biodegradation, BPA concentrations from 100 to 100,000 ng L^{-1} and from 1 to 100 ng L^{-1} have respectively reported in influent and effluent streams from several WWTPs worldwide [30].

Conventional physical–chemical or biological processes are unable to remove BPA from water [31]. Therefore, several AOPs such as CWPO [32-34], Fenton/photo-Fenton oxidation [35-37], sonochemical treatment [38], photochemical/photocatalytic oxidation [39-42], ozonation [43], and hybrid processes [44-48] have been tested.

The aim of this study is to prepare iron catalysts supported on grape seeds-derived carbon materials and to test them in CWPO using BPA as target compound. The fresh and used catalysts have been characterized by several techniques including CO_2 adsorption at 273 K, elemental analysis, ash content, total reflection X-ray fluorescence spectroscopy (TXRF), X-ray photoelectron spectroscopy (XPS) and Scanning Electron Microscopy - Energy Dispersive X-ray spectroscopy (SEM-EDX). The CWPO results have been analyzed in terms of H_2O_2 decomposition, BPA removal and TOC conversion. Additionally, the toxicity and biodegradability of BPA and the CWPO effluent were evaluated. The stability of the most interesting catalyst was also tested in long-term continuous operation (100 h on stream).

2. Material and methods

2.1 Catalysts preparation and characterization

The grape seeds used as precursor were from the red wine variety "Tinta de Toro" harvested in Toro (Zamora, Spain). The sizes of the raw seeds were between 2 and 4 mm. The seeds were washed with distilled water, dried at 105 ºC for 24 h and pyrolyzed in a rotatory quartz furnace (CARBOLITE CB HTR 11/150P8) at 600 ºC for 2 h [2]. The working temperature was reached at a 10 ºC min^{-1} heating rate and N_2 was continuously passed at a 1 NL min^{-1} flow rate. The resulting char is identified as GS-0. It was activated with air (2 NL min^{-1}) for 2 h at 400 ºC, reached at 10 ºC min^{-1} [6]. This activated carbon was named GS-1. The GS-0 char was also subjected to oxidative treatment with HNO_3 which was carried out boiling 1 g of char in 10 mL of a 6 N HNO_3 solution for 20 min followed by washing with distilled water until neutral pH [49]. This oxidized carbon was identified as GS-2. The HNO_3 oxidation treatment was also applied to the air-activated carbon giving rise to the GS-3 carbon. Iron was incorporated on each carbon support by incipient wetness impregnation with an aqueous solution of $Fe(NO_3)\cdot 9H_2O$ (Panreac, 97%) to obtain catalysts with a 4.0 % wt. of Fe. Once impregnated, each catalyst was dried at 60 ºC for 12 h and calcined for 4 h at 300 ºC, reached at 3ºC min^{-1}. The catalysts, with granular morphology, were identified adding Fe to the name of the support (Fe-GS-1, Fe-GS-2 and Fe-GS-3).

The surface area and total pore volume of the catalysts were determined by CO_2 adsorption at 0 ºC in an automated volumetric gas adsorption apparatus (MicromeriticsTristar 3020). Previous to adsorption the samples (0.15 g) were degasified under vacuum at 150 ºC for 7 h using a degas system (Micromeritics VacPrep 061). The surface area (S_{DA}) and the micropore volume ($V_{microCO2}$, 0.4–0.9 nm) were calculated using the Dubinin–Astakhov equation. This approach was used because materials with narrow microporosity were expected according to previous works [2,6]. The pH slurry was determined measuring, until constant value, the pH of an aqueous suspension of catalyst (1 g) in distilled water (10 mL). The morphology of the catalyst and its surface composition were analyzed by Scanning Electron Microscopy - Energy

Dispersive X-ray spectroscopy (SEM-EDX) with a Hitachi S-3000N apparatus. The samples for SEM observation were metalized with gold using a Sputter Coater SC502. Imaging was performed in the high vacuum mode under an accelerating voltage of 20 kV, using secondary and backscattered electrons. Elemental analyses (C, N, S, and H) were carried out with a LECO CHNS-932 analyzer, while the ash content was determined following the standard ASTM D1506-99 method. The oxygen content was calculated by difference to 100%. Moreover, catalyst surface composition was quantified by X-ray photoelectron spectroscopy (XPS) using a 5700C model Physical Electronics apparatus, with MgKα radiation (1253.6 eV) and energy dispersive X-ray spectroscopy analysis (EDAX). The bulk Fe loading was determined by total reflection X-ray fluorescence spectroscopy (TXRF), using Si-Li detector in a TXRF Extra-II Rich & Seifert spectrometer.

2.2. CWPO experiments

The CWPO runs were carried out in glass-made stirred batch reactors at atmospheric pressure, 600 rpm stirring velocity and temperatures within 50 - 80 ºC for 4 h. Duplicate runs were always made. The starting concentration of BPA (Sigma-Aldrich, >99%) was 100 mg L^{-1}, the H_2O_2 (Panreac, 33%w/v) doses were 265 and 530 mg L^{-1}, which correspond, respectively, to 50 and 100 % of the theoretical stoichiometric amount for complete oxidation of BPA to CO_2 and H_2O (mineralization). The catalyst concentration was fixed at 500 mg L^{-1}. The initial pH was adjusted to 3.0 with nitric acid and continuously monitored along the experiment. A set of experiments were carried out to check the H_2O_2 decomposition (50ºC, 530 mg L^{-1} H_2O_2 and 500 mg L^{-1} catalyst), and the adsorption of BPA on the catalysts in absence of H_2O_2 (50 and 80ºC, 100 mg L^{-1} BPA and 500 mg L^{-1} catalyst). Long-term experiments (100 h on stream) were performed in a continuous stirred tank reactor (CSTR) fed with BPA (200 mg L^{-1}) and H_2O_2 (1060 mg L^{-1}) aqueous solutions at 2 ml min^{-1} of each reactant. A catalyst loading of 500 mg L^{-1} was always used, so that the space-time (τ) was fixed at 4.7 kg_{cat} h mol_{BPA}^{-1}. These experiments were performed at 80 ºC, atmospheric pressure and 600 rpm stirring velocity.

The process was followed by analyzing periodically samples from the batchwise experiments or from the exit stream in the continuous ones. BPA and aromatic intermediates were quantified by means of high performance liquid chromatography (HPLC) with an UV-Vis detector (Varian). BPA and 4-hydroxyacetophenone (4-HAP) were analyzed using a Microsorb-MV 100-5 C18 column with 1 mL min^{-1} of a gradient of methanol-water (46 to 90 % of methanol) as mobile phase at 225 and 275 nm, respectively. For the aromatic intermediates a Microsorb-MV 100-5 C18 column was used with an aqueous sulphuric solution (0.1 M) as mobile phase at 210 nm wavelength for hydroquinone (HQ) and at 246 nm for *p*-benzoquinone (BQ). Ion chromatography with chemical suppression (Metrohm 790 Personal IC) was employed to detect short-chain organic acids (acetic and maleic acids) using a METROSEP A Supp 5 250/4.0 column with 0.7 mL min^{-1} of 1.0 mM $NaHCO_3$/3.2 mM Na_2CO_3 as mobile phase. Total organic carbon was measured with a TOC Analyzer (Shimadzu TOC-VCSH). H_2O_2 was analyzed by colorimetric titration using a UV/Vis spectrophotometer (Cary 60, Agilent) from the formation of Ti(IV) - H_2O_2 complex, which was quantified at 410 nm [50]. The iron leached to the liquid phase was measured by colorimetric titration at 510 nm using the o-phenatroline method [51].

Ecotoxicity of the initial BPA solution and the reaction effluents was determined by the Microtox® Acute Toxicity Test (SCI 500 Analyzer) which measures the percent decrease of the light emission of *Vibrio fischeri* after 15 min of incubation at 15 ºC, adjusting the osmotic pressure of the samples close to 2% NaCl and pH between 6 and 8. The ecotoxicity values were expressed as EC_{50} for BPA, defined as the effective concentration of a sample that causes 50% reduction of bioluminescence, or IC_{50} for the reaction samples, defined as the dilution ratio (%) of the sample that yields this 50% light emission reduction. The IC_{50} values are inversely proportional to ecotoxicity expressed in toxicity units (TU).

Toxicity was also evaluated using the method proposed by Polo et al. [52], based on the OECD 209 respiration inhibition test for activated sludge. This procedure consisted on the use of an unacclimated sludge in short-term respirometric measurements in contact with BPA at different concentrations in the presence of an easily biodegradable compound, such as sodium acetate.

Inhibition was also estimated in terms of EC_{50}, defined as the concentration of the toxicant causing a 50% reduction of the exogenous SOUR (specific oxygen uptake rate) obtained in the presence of sodium acetate as sole carbon source. The biodegradability assays were carried out following the typical operating conditions of an activated sludge process, measuring toxicant removal and the activity of microorganisms [52,53]. In a close reactor were incorporated the unacclimated sludge and the target compound, and the SOUR profile was obtained interrupting the air supply and measuring the dissolved oxygen decay in a range of 0.3 mg L^{-1}. The tests were carried out for 24 h at 25 ºC. Biodegradation was followed from the evolution of BPA and TOC.

3. Results and discussion

3.1. Catalyst Characterization

Table 1 summarizes the characterization of the raw seed, the char resulting from pyrolysis, the activated carbons used as supports and the corresponding Fe catalysts. The pyrolysis caused a 1.5-fold increase of the C percentage with respect to the raw grape seed. In terms of elemental analysis, the N content was somewhat higher in GS-2 and GS-3, and consequently, in Fe-GS-2 and Fe-GS-3 due to the treatment with HNO_3. Furthermore, this treatment, that creates surface oxygenated groups [49,54], increased also the surface acidity as can be inferred from the pH_{slurry} values of 5.6 and 6.1 for Fe-GS-2 and Fe-GS-3, respectively, versus 7.9 for Fe-GS-1 catalyst. Regarding the specific surface area, pyrolysis led to a char with S_{DA} around 400 m^2 g^{-1}, with a significant development of microporosity (micropore volume close to 0.14 cm^3 g^{-1}). Air activation produced a low increase of surface area, whereas the HNO_3 treatment lowered the S_{DA} of the char. Air-activation followed by HNO_3 treatment led to the highest surface area (484 m^2 g^{-1}) and pore volume (0.166 cm^3 g^{-1}). The bulk iron content indicates that the Fe incorporation in Fe-GS-1 catalyst (2.8 %wt.) was less effective than in the other two catalysts, where the expected content of around 4 % wt. was more closely achieved and even surpassed (Fe-GS-3). This fact can be explained by the presence of surface oxygenated groups which can favor the Fe uptake. The values of the Fe_{XPS}/Fe_{Bulk} ratio, frankly higher than 1, are indicative of

a heterogeneous distribution of the metal phase, a predominant location on the outermost surface, most pronounced in the case of the two catalyst supported on air-activated carbons (Fe-GS-1 and Fe-GS-3). Air activation creates surface oxygenated groups which may favor the preferential location of Fe on the external or non-microporous surface rather than in the internal microporosity.

The original granular structure and the size (around 2-4 mm) of the grape seeds were maintained in the char from pyrolysis as confirmed by SEM. Occasionally the internal overpressure during pyrolysis can cause some opening of the coat [2,9]. Figure 1 presents SEM images of entire and broken particles of the Fe-GS catalysts showing iron distribution. In the case of the Fe-GS-1 catalyst (Figure 1.A) the iron particles were mainly found on the outer surface. The Fe-GS-2 catalyst SEM image (Figure 1.B) showed that there is less active phase on the external surface, since iron was found inside the support. Finally, the Fe-GS-3 catalyst micrograph (Figure 1.C) shows an outer layer of iron, as well as, a thin layer of the same on the inside surface. As representative example, Figure 1.D shows the energy dispersive X-ray spectrum (EDX) of the Fe-GS-1 catalyst. Similar profiles were obtained for the other catalysts.

3.2. CWPO experiments

Previous blank tests were carried out in order to learn on the possible thermal decomposition of H_2O_2 in the presence of BPA without catalyst under the operating conditions to be used in the CWPO experiments. H_2O_2 decomposition was lower than 5 % and no changes were observed in the BPA concentration. Adsorption of BPA onto the catalysts in absence of H_2O_2 was checked. At 50ºC the adsorption capacity of BPA was lower than 20 mg_{BPA} g^{-1} for Fe-GS-1 and Fe-GS-3 catalysts and around 4 mg_{BPA} g^{-1} for Fe-GS-2, while at 80 ºC it was negligible in all the catalysts (< 2 mg_{BPA} g^{-1}).

The activity of the catalyst for H_2O_2 decomposition in absence of BPA was tested. Figure 1 shows the evolution of H_2O_2 upon time reaction. The data were adjusted to a pseudo first-order rate equation, a simple approach which serves to describe the kinetics of H_2O_2 decomposition

with activated carbon [55]. The reaction with the Fe-GS-2 catalyst yield the lowest kinetic constant (10^{-4} min^{-1}) whereas values of $7 \cdot 10^{-4}$ and $1.1 \cdot 10^{-3}$ min^{-1} were obtained with Fe-GS-3 and Fe-GS-1, respectively.

Table 2 shows the results from CWPO of BPA at 50 ºC with the three catalysts tested. The pH remained almost unchangeable (≈ 3) along the experiment in all the cases. The Fe-GS-1 and Fe-GS-3 catalysts achieved complete BPA conversion. The second required some more time due to an initial induction period of 60 min, where a lower H_2O_2 decomposition took place. On the other hand, the Fe-GS-2 showed low BPA removal with no TOC reduction and a negligible H_2O_2 conversion. This indicates that the treatment with HNO_3 is insufficient to obtain an active catalyst under these operating conditions. The Fe-GS-1 catalyst allowed somewhat higher TOC reduction than Fe-GS-3, consistently with the higher percentage of H_2O_2 decomposition. However, in both cases, the extent of mineralization was fairly low and a high relative amount of H_2O_2 remained after 4 h (more than 65% of the initial). Therefore, the operating conditions were insufficient for an acceptable mineralization of BPA. Aromatic reaction intermediates (4-HAP, HQ and BQ) were detected at concentrations below 1 mg L^{-1} and short-chain acids, such as acetic and maleic acid, at concentrations below 15 mg L^{-1}.

From the results so far, Fe-GS-1 catalyst was selected to analyze the influence of the operating conditions (T and H_2O_2 concentration) on the CWPO process. Figure 3 shows the time-course of H_2O_2 concentration and BPA conversion as well as TOC and dissolved Fe concentration at different temperatures and H_2O_2 doses. In all the cases complete conversion of BPA was reached, even though the H_2O_2 decomposition after 4 h of reaction was not complete. The increase of the temperature led to a higher rate of disappearance of BPA and higher mineralization. At 80 ºC, with the stoichiometric amount of H_2O_2 (530 mg L^{-1}) complete conversion of BPA was achieved in 30 min and once H_2O_2 was depleted (≈ 180 min) TOC reduction was close to 65 %. The TOC reduction reached a plateau-like level, corresponding to the residual species essentially to light organics acids, mostly the acetic, highly resistant to this treatment. The concentration of Fe in solution was negligible up to around 120 min of reaction.

By that time BPA was completely disappeared, mineralization was about 50 % and 90 % H_2O_2 was already decomposed. Thus, the possible contribution of dissolved Fe can be considered of very low significance, if any. Cleveland et al. [34] observed that the CWPO of BPA using carbon nanotube-supported Fe_3O_4 was enhanced by 3.5 when the temperature increased from 20 ºC to 50 ºC, achieving high rates of BPA degradation and a COD removal efficiency around 40 %. However, the efficiency on the use of H_2O_2 (amount of TOC removed per unit of H_2O_2 decomposed) remained almost inalterable at around 0.10 mg_{TOC} mg_{H2O2}^{-1} after the 240 min of the experiment without significant variation with temperature and the H_2O_2 dose within the range of values tested.

Regarding to Fe leaching, its presence in the liquid phase was not detected up to 120 min reaction time. It increased with the temperature but did not exceed 5 % of the initial Fe load of the catalyst at the end of the experiment. Previous works have related the Fe leaching with the presence of oxalic acid [12,14], but in this study that species was not detected in any case.

3.3. Ecotoxicity and biodegradability experiments

A value of EC_{50} of 4.2 mg L^{-1} was obtained for BPA by the Microtox Toxicity Test. The EC_{50} reported in the literature [56] range from 1.0 to 10 mg L^{-1}, so BPA is classified as “moderately toxic” and “toxic” to aquatic biota by the European Commission and the United States Environmental Protection Agency (US EPA). The EC_{50} value obtained by the respiration inhibition test with activated sludge was 47 mg L^{-1}. According to these values, Microtox Test resulted more sensitive to BPA than the activated sludge as concluded Polo et al. (2011), who reported that the Microtox® test overestimates the potential negative effect on the activated sludge of a wastewater treatment plant [52].

A sample of the initial and final effluent from CWPO of BPA at 80 ºC with Fe-GS-1 using the stoichiometric H_2O_2 dose was subjected to the Microtox Test. The toxicity of initial solution was of 23.8 TU, whereas the final effluent yield almost negligible ecotoxicity.

BPA can be considered as no readily biodegradable since no changes on the concentration of BPA and TOC nor significant variations of SOUR were detected along the biodegradability test (Figure 4A). The results of that test with a sample of CWPO effluent are depicted in Figure 4B. The respirometric profile shows an increase of sludge respiration at three intervals of time associated with the degradation of the by-products from CWPO of BPA (acetic and maleic acid). More than 40% of TOC reduction was observed. Previous works have reported that acetic acid is the most readily biodegradable compound among the identified oxidation by-products whereas maleic acids require an acclimation time of the sludge [57,58].

3.6. Stability of the catalyst

The evaluation of the stability in long-term experiments is critical for the practical application of CWPO processes. To address catalyst stability, a long-term experiment was carried out in a continuous stirred tank reactor at 80 ºC at 4.7 kg_{cat} h mol_{BPA}^{-1} space-time. Figure 5 shows the evolution of BPA and TOC conversion upon time on stream. The TOC reduction decreased from 46 % at 6 h to 30 % at 15 h and then remained almost constant. A similar trend was observed for BPA conversion, which decrease during the initial 10 h on stream but then remained at about 90 % up to the end of the 100 h – experiment. This initial loss of activity can be due to Fe leaching, which was detected only during the initial 10 h on stream. As reaction by products were identified 4-HAF, BQ, maleic acid and acetic acid. The two last achieved maximum concentrations at around 15 h on stream and then stabilized in the vicinity of 10 mg L^{-1} each. Almost constant residual concentrations of aromatic intermediates (4-HAP and BQ) were maintained upon the whole experiment. Those species require working at higher space-time than that of the experiments for complete disappearance, a crucial issue in particular in the case of BQ, given its high ecotoxicity. TXRF analyses of the effluent showed that Fe leaching was around 20% after 100 h, mainly occurring within the early stages on stream. The characterization of the used catalyst did not show significant changes in terms of S_{DA}, micropores volume or elemental analysis.

4. **Conclusions**

Three Fe catalysts were prepared using grape seeds-derived activated carbons as supports. The catalysts were tested in CWPO of bisphenol A. They were microporous materials with CO_2 measured surface area values in the range of ≈ 350-500 m^2 g^{-1} and with the Fe located mainly at the outermost surface. The catalyst with 2.8 % Fe over air-activated carbon showed the best performance, allowing complete conversion of BPA and TOC reduction up to 60 % at 80 ºC with the stoichiometric amount of H_2O_2 in less than 3 h reaction time. Moreover, this treatment provoked a dramatic reduction of the ecotoxicity and a significant improvement of the biodegradability. In long-term operation (100 h on stream), Fe-GS-1 catalyst suffered a loss of activity upon the early stages (≈ 15 h), probably associated to the observed Fe leaching (around 20 % of the initial load). Then the catalyst showed a fairly stable behavior. The characterization of the used catalyst did not revealed any significant changes in terms of porous texture and elemental composition.

Acknowledgements

The authors wish to thank the Spanish MINECO and Comunidad de Madrid for the financial support through the projects CTM2013-43803-P and S2013/MAE-2716, respectively. I. F. Mena wishes to thank the MINECO and the ESF for a research grant.

References

[1] D. Savova, E. Apak, E. Ekinci, F. Yardim, N. Petrov, T. Budinova, M. Razvigorova, V. Minkova. Biomass conversion to carbon adsorbents and gas. Biomass Bioenerg. 21 (2001) 133–142.

[2] D. Jimenez-Cordero, F. Heras, N. Alonso-Morales, M.A. Gilarranz, J.J. Rodriguez. Porous structure and morphology of granular chars from flash and conventional pyrolysis of grape seeds. Biomass Bioenerg. 54 (2013) 123-132.

[3] K. Gergova, N. Petrov, S. Eser. Adsorption properties and microstructure of activated carbons produced from agricultural by-products by steam pyrolysis. Carbon 32 (1994) 693–702.

[4] J. M. Encinar, F. J. Beltran, A. Bernalte, A. Biro and J. F. Gonzalez. Pyrolysis of two agricultural residues: olive and grape bagasse. Influence of particle size and temperature. Biomass Bioenerg. 11 (1996) 397–409.

[5] S. Uçar, S. Karagöz. The slow pyrolysis of pomegranate seeds: The effect of temperature on the product yields and bio-oil properties. J. Anal. Appl. Pyrolysis 84 (2009) 151–156.

[6] D. Jimenez-Cordero, Francisco Heras, M. A. Gilarranz, E. Raymundo-Piñero. Grape seed carbons for studying the influence of texture on supercapacitor behaviour in aqueous electrolytes. Carbon 71 (2014) 127–138.

[7] M. Al Bahri, L. Calvo, M.A. Gilarranz, J.J. Rodriguez. Activated carbon from grape seeds upon chemical activation with phosphoric acid: Application to the adsorption of diuron from water. Chem. Eng. J. 203 (2012) 348–356.

[8] M. Al Bahri, L. Calvo, A.M. Polo, M.A. Gilarranz, A.F. Mohedano, J.J. Rodriguez. Identification of by-products and toxicity assessment in aqueous-phase hydrodechlorination of diuron with palladium on activated carbon catalysts. Chemosphere 91 (2013) 1317-1323.

[9] M. Al Bahri, L. Calvo, M.A. Gilarranz, J.J Rodriguez, F. Epron. Activated carbon supported metal catalysts for reduction of nitrate in water with high selectivity towards N_2. Appl. Catal. B: Environ. 138– 139 (2013) 141– 148.

[10] E. Neyens, J. Baeyens, A review of classic Fenton's peroxidation as an advanced oxidation technique, J. Hazard. Mater. 98 (2003) 33–50.

[11] J.J. Pignatello, E. Oliveros, A. MacKay, Advanced oxidation processes for organic contaminant destruction based on the Fenton reaction and related chemistry, Crit. Rev. Environ. Sci. Technol. 36 (2006) 1–84.

[12] P. Bautista, A.F. Mohedano, J.A. Casas, J.A. Zazo, J.J. Rodriguez. Highly stable Fe/γ -Al_2O_3 catalyst for catalytic wet peroxide oxidation. J. Chem. Technol. Biotechnol. 83 (2008) 1323.

[13] N. Inchaurrondo, J. Cechinia, J. Font, P. Haure. Strategies for enhanced CWPO of phenol solutions. Appl. Catal. B: Environ. 111– 112 (2012) 641– 648.

[14] J.A. Zazo, J. Bedia, C.M. Fierro, G. Pliego, J.A. Casas, J.J. Rodriguez. Highly stable Fe on activated carbon catalysts for CWPO upon $FeCl_3$ activation of lignin from black liquors. Catal. Today 187 (2012) 115– 121.

[15] A.F. Mohedano, V.M. Monsalvo, J. Bedia, J. Lopez, J.J. Rodríguez. Highly stable iron on carbon catalysts obtained from sewage sludge for CWPO. J. Environ. Chem. Eng. 2 (2014) 2359–2364.

[16] D.J. Doocey, P.N. Sharratt, Zeolite-mediated advanced oxidation of model chlorinated phenolic aqueous waste: Part 1: Aqueous phase Fenton catalysis, Process Saf. Environ. Prot. 82 (2004) 352–358.

[17] R.S. Ribeiro, A.M.T. Silva, L.M. Pastrana-Martínez, J.L. Figueiredo, J.L. Fariab, H.T. Gomes. Graphene-based materials for the catalytic wet peroxide oxidation of highly concentrated 4-nitrophenol solutions. Catal. Today 249 (2015) 204–212.

[18] J.A. Zazo, J.A. Casas, A.F. Mohedano, J.J. Rodriguez. Catalytic wet peroxide oxidation of phenol with a Fe/active carbon catalyst. Appl. Catal. B: Environ. 65 (2006) 261–268.

[19] S. A. Messele, F. Stüber, C. Bengoa, A. Fortuny, A. Fabregat, J. Font. Phenol degradation by heterogeneous Fenton-like reaction using Fe supported over activated carbon. Procedia Eng. 42 (2012) 1373–1377.

[20] S. A. Messele, O.S.G.P. Soares, J.J.M. Órfão, F. Stüber, C. Bengoa, A. Fortuny, A. Fabregat, J. Font. Zero-valent iron supported on nitrogen-containing activated carbon for catalytic wet peroxide oxidation of phenol. Appl. Catal. B: Environ. 154–155 (2014) 329–338.

[21] J. Barrault, J.M. Tatibouet, N. Papayannakos. Catalytic wet peroxide oxidation of phenol over pillared clays containing iron or copper species. Chem. 3 (2000) 777–783.

[22] R. S. Ribeiro, A. M. T. Silva, J. L. Figueiredo, J. L. Faria, H. T. Gomes. Catalytic wet peroxide oxidation: a route towards the application of hybrid magnetic carbon nanocomposites for the degradation of organic pollutants. A review. Appl. Catal. B: Environ. 187 (2016) 428–460.

[23] M. Umar, F. Roddick, L. Fan, H. A. Aziz. Application of ozone for the removal of bisphenol A from water and wastewater – A review. Chemosphere 90 (2013) 2197–2207.

[24] J. R. Rochester. Bisphenol A and human health: A review of the literature. Reprod. Toxicol. 42 (2013) 132– 155.

[25] Y. Yang, Z. Wang, S. Xie. Aerobic biodegradation of bisphenol A in river sediment and associated bacterial community change. Sci. Total Environ. 470–471 (2014) 1184–1188.

[26] D. D. Seachrist, K. W. Bonk, S. Ho, G. S. Prins, A. M. Soto, R. A. Keri. A review of the carcinogenic potential of bisphenol A. Reprod. Toxicol. 59 (2016) 167-182.

[27] M. Furhacker, S. Scharf, H. Weber. Bisphenol A: emission from point sources. Chemosphere 41 (2000), 751–756.

[28] C. A. Staples, P.B. Dorn, G.M. Klecka, S.T. Oblock, L.R. Harris. A review of the environmental fate, effects and exposures of Bisphenol A. Chemosphere 36 (1998), 2149–2173.

[29] T. Yamamoto, A. Yasuhara, H. Shiraishi, O. Nakasugi. Bisphenol A in hazardous waste landfill leachates. Chemosphere 42 (2001), 415–418.

[30] H. Melcer, G. Klecka. Treatment of Wastewaters Containing Bisphenol A: State of the Science Review. Water Environ. Res. 83 (2011) 650-666.

[31] I. Gültekin, N.H. Ince. Synthetic endocrine disruptors in the environment and water remediation by advanced oxidation processes. J. Environ. Manage. 85 (2007), 816–832.

[32] X.J. Yang, X.M. Xu, X.C. Xu, J. Xu., H.L. Wang, R. Semiat, Y.-F. Han. Modeling and kinetics study of Bisphenol A (BPA) degradation over an $FeOCl/SiO_2$ Fenton-like catalyst. Catal. Today (2016), doi:10.1016/j.cattod.2016.01.002.

[33] J. Du, J. Bao, X. Fu, C. Lu, S. H. Kim. Mesoporous sulfur-modified iron oxide as an effective Fenton-like catalyst for degradation of bisphenol A. Appl. Catal. B: Environ. 184 (2016) 132–141.

[34] V. Cleveland, J. Bingham, E. Kann. Heterogeneous Fenton degradation of bisphenol A by carbon nanotube-supported Fe_3O_4. Sep. Purif. Tech. 133 (2014) 388–395.

[35] H. Katsumata, S. Kawabe, S. Kaneco, T. Suzuki, K. Ohta. Degradation of bisphenol A in water by the photo-Fenton reaction. J. Photochem. Photobiol. A: Chem., 162 (2004), 297–305.

[36] W. T. Tsai, M. K. Lee, T. Y. Su, Y. M. Chang. Photodegradation of bisphenol-A in a batch TiO_2 suspension reactor. J. Hazard. Mater. 168 (2009) 269–275.

[37] J. Poerschmann, U. Trommler, T. Gorecki. Aromatic intermediate formation during oxidative degradation of Bisphenol A by homogeneous sub-stoichiometric Fenton reaction. Chemosphere, 79 (2010), 975–986.

[38] K. Zhang, N. Gao, Y. Deng, T.F. Lin, Y. Ma, M. Sui. Degradation of Bisphenol-A using ultrasonic irradiation assisted by low concentration hydrogen peroxide. J. Environ. Sci., 23 (2011), 31–36.

[39] M. Bistan, T. Tisler, A. Pintar. Catalytic and photocatalytic oxidation of aqueous bisphenol A solutions: removal, toxicity, and estrogenicity. Ind. Eng. Chem. Res., 51 (2012), 8826–8834.

[40] H. Dimitroula, V. M. Daskalaki, Z. Frontistis, D. I. Kondarides, P. Panagiotopoulou, N. P. Xekoukoulotakis, D. Mantzavinos. Solar photocatalysis for the abatement of emerging micro-contaminants in wastewater: Synthesis, characterization and testing of various TiO_2 samples. Appl. Catal. B: Environ. 117–118 (2012) 283–29.

[41] S.H. Yoon, S. Jeong, S. Lee. Oxidation of bisphenol A by UV/$S_2O_8^{2-}$: comparison with UV/H_2O_2. J. Environ. Technol., 33 (2012), 123–128.

[42] J. Zhang, B. Sun, X. Guan. Oxidative removal of bisphenol A by permanganate: kinetics, pathways and influences of co-existing chemicals. Sep. Purif. Technol., 107 (2013), 48–53.

[43] J. Lee, H. Park, J. Yoon. Ozonation characteristics of bisphenol A in water. Environ. Technol., 24 (2003), 241–248.

[44] R.A. Torres, C. Petrier, E. Combet, F. Moulet, C. Pulgarin. Bisphenol A mineralization by integrated ultrasound-UV-iron (II) treatment. Environ. Sci. Technol., 41 (2006), 297–302;

[45] Y-F. Huang, Y-H. Huang. Identification of produced powerful radicals involved in the mineralization of bisphenol A using a novel UV-$Na_2S_2O_8$/H_2O_2-Fe(II, III) two-stage oxidation process. J. Hazard. Mater., 162 (2009), 1211–1216.

[46] Z. Frontistis, V. M. Daskalaki, A. Katsaounis, I. Poulios, D. Mantzavinos. Electrochemical enhancement of solar photocatalysis: Degradation of endocrine disruptor bisphenol-A on Ti/TiO_2 films. Water Res. 45 (2011) 2996–3004.

[47] J. Sharma, I.M. Mishra, D.D. Dionysiou, V. Kumar. Oxidative removal of Bisphenol A by UV-C/peroxymonosulfate (PMS): Kinetics, influence of co-existing chemicals and degradation pathway. Chem. Eng. J., 276, 15, (2015), 193–204.

[48] B. Darsinou, Z. Frontistis, M. Antonopoulou, I. Konstantinou, D. Mantzavinos. Sono-activated persulfate oxidation of bisphenol A: Kinetics, pathways and the controversial role of temperature Chem. Eng. J. 280 (2015) 623–633.

[49] A. Gil, G. de la Puente, P. Grange. Evidence of textural modifications of an activated carbon on liquid-phase oxidation treatments. Microporous Mater. 12 (1997) 51-61.

[50] G.M. Eisenberg. Colorimetric determination of hydrogen peroxide. Ind. Eng. Chem., Anal. Ed. 15 (1943) 327-328.

[51] E.B. Sandell. Colorimetric Determination of Traces of Metals, third ed., Interscience Pubs, New York, 1959.

[52] A.M. Polo, M. Tobajas, S. Sanchis, A.F. Mohedano, J.J. Rodriguez. Comparison of experimental methods for determination of toxicity and biodegradability of xenobiotic compounds. Biodegradation 22 (2011) 751-761.

[53] E. Diaz, A.M. Polo, A.F. Mohedano, J.A. Casas, J.J. Rodriguez. On the biodegradability of nitrophenols and their reaction products by catalytic hydrogenation. J. Chem. Technol. Biotechnol. 87 (2012) 1263-1269.

[54] L. Calvo, A.F. Mohedano, J.A. Casas, M.A. Gilarranz, J.J. Rodriguez, J. J. Treatment of chlorophenols-bearing wastewaters through hydrodechlorination using Pd/activated carbon catalysts. Carbon 42 (2004) 1377-1381.

[55] A. Rey, J.A. Zazo, J.A. Casas, A. Bahamonde, J.J. Rodriguez. Influence of the structural and surface characteristics of activated carbon on the catalytic decomposition of hydrogen peroxide. Appl. Catal. A: Gen. 402 (2011) 146– 155.

[56] Alexander, H.C., Dill, D.C., Smith, L.W., Guiney, P.D., Dorn, P., 1988. Bisphenol A: acute aquatic toxicity. Environ. Toxicol. Chem. 7, 19-26.

[57] C.B. Molina, A.H. Pizarro, V.M. Monsalvo, A.M. Polo, A.F. Mohedano, J.J. Rodriguez. Integrated CWPO and biological treatment for the removal of 4-chlorophenol from water. Sep. Sci. Technol. 45 (2010) 1595- 1602.

[58] V.M. Monsalvo, J. Lopez, M. Munoz, Z.M. de Pedro, J.A. Casas, A.F. Mohedano, J.J. Rodriguez. Application of Fenton-like oxidation as pre-treatment for carbamazepine biodegradation. Chem. Eng. J. 264 (2015) 856-862.

Figure captions

Figure 1. SEM images of the entire, half-broken and the surfaces of the Fe-GS catalysts. Fe-GS-1 (A), Fe-GS-2 (B) y Fe-GS-3 (C) and EDX spectra of Fe-GS-1 (D).

Figure 2. Hydrogen peroxide decomposition whit the Fe-GS catalysts ($[H_2O_2]_o$: 530 mg L^{-1}, T: 50 ºC, pH_o: 3).

Figure 3. CWPO of BPA with the Fe-GS-1 catalyst at the stoichiometric (A,B) and half-stoichiometric (C,D) H_2O_2 doses vs reaction time at different temperatures. BPA and TOC conversion: solid symbols; H_2O_2 concentration: open symbols. Insert: dissolved Fe.

Figure 4. Time course of BPA and TOC, and respirometric profiles obtained in the fast biodegradability test for a BPA watersolution (A) and the resulting effluent from CWPO (B).

Figure 5. Long-term performance of the catalyst upon CWPO of BPA ([BPA]: 100 mg L^{-1}, $[H_2O_2]$: 530 mg L^{-1}, T: 80 ºC, pH_o: 3, τ: 4.7 kg_{cat} h mol^{-1}_{BPA}).

Figure 1

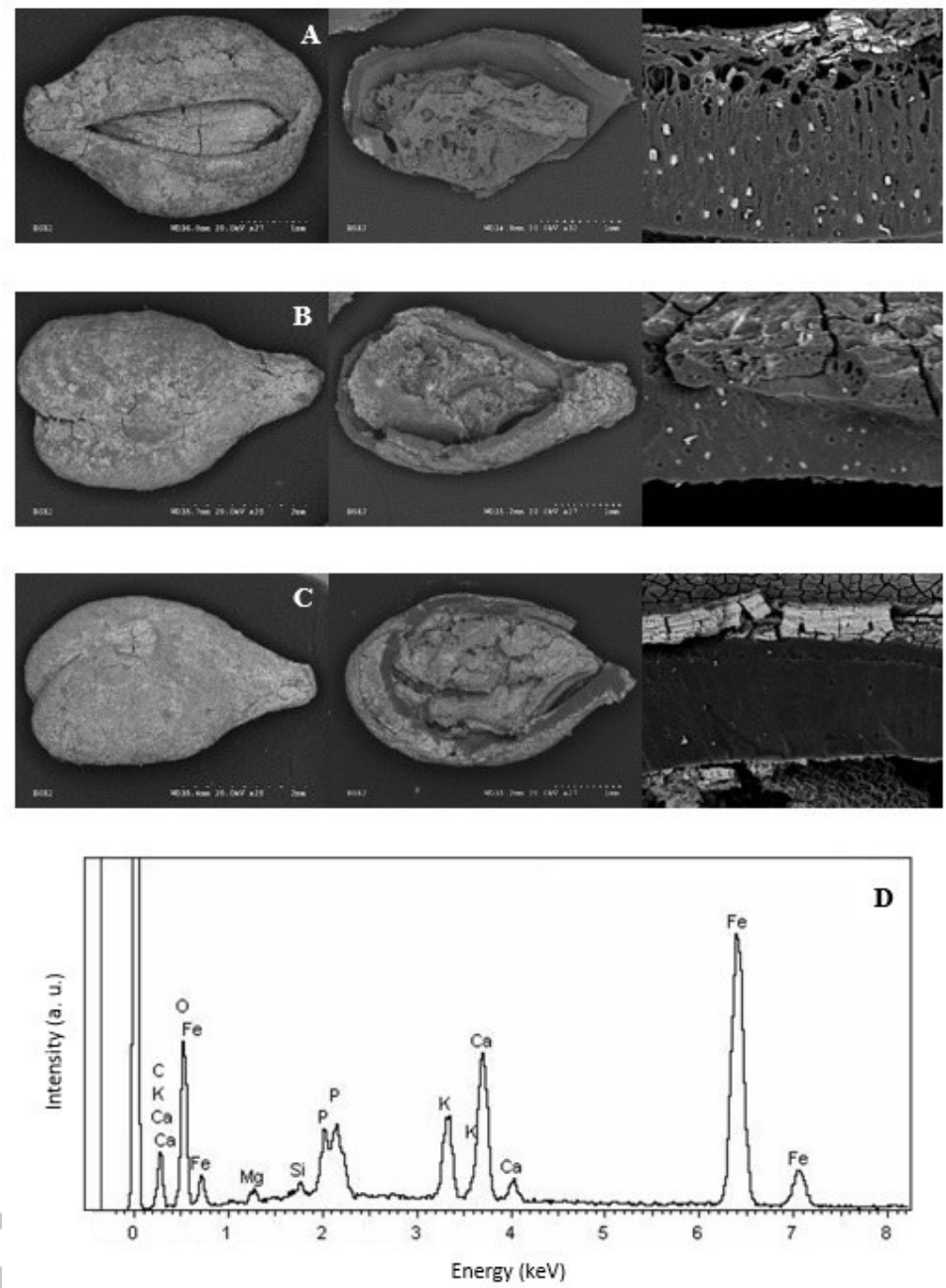

Figure 2

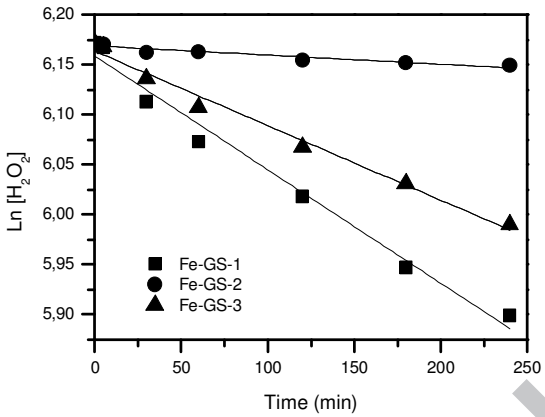

Figure 3

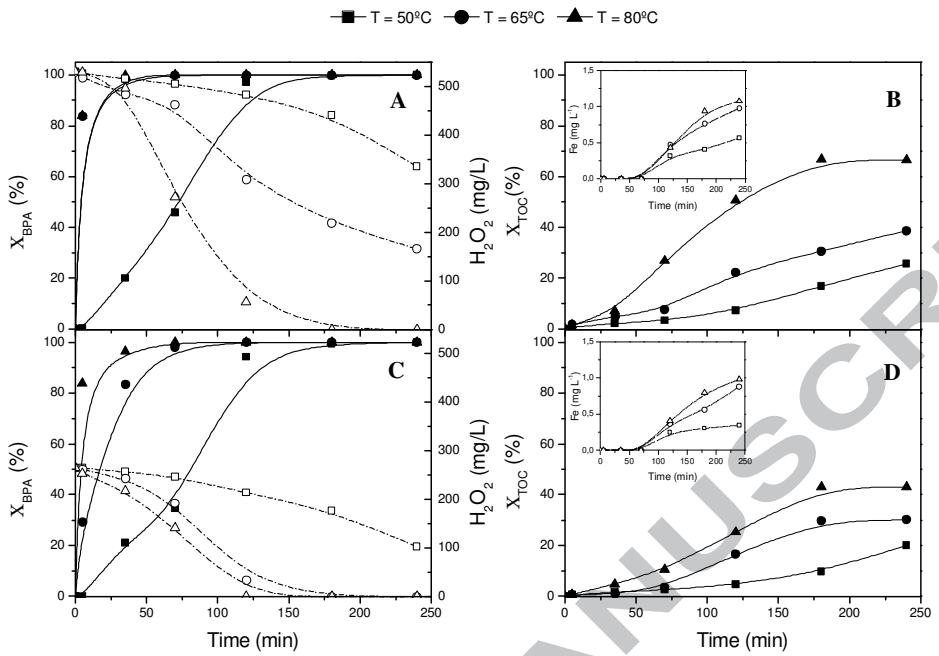

Figure 4

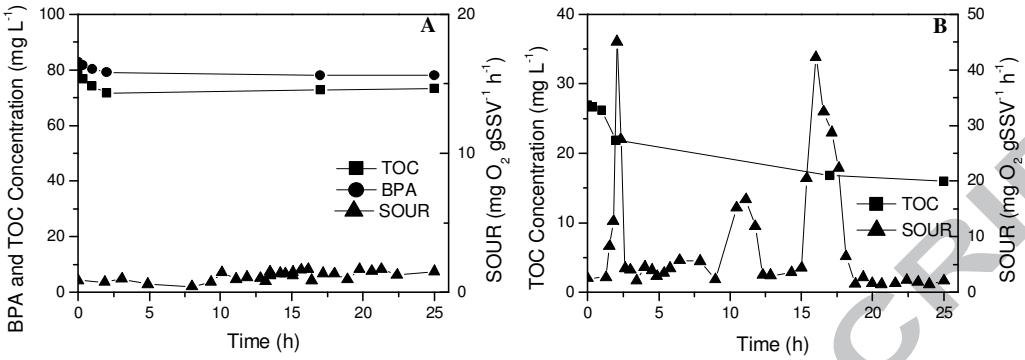

Figure 5

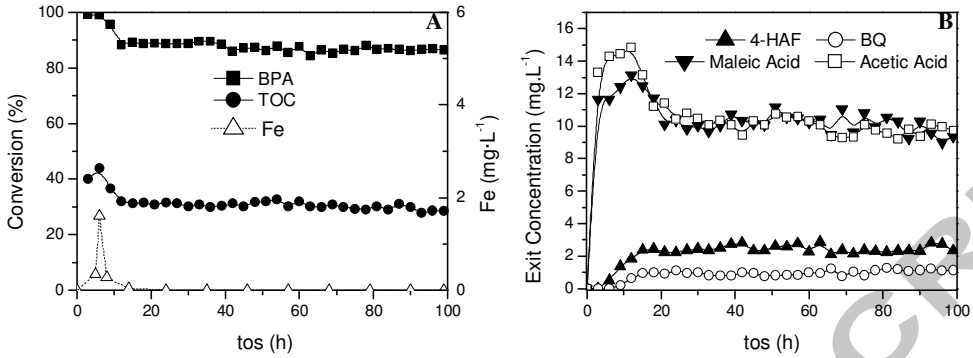

Table 1. Characterization of the raw seeds (GS), the char (GS-0), carbon supports (GS) and Fe catalysts (Fe-GS).

Material	Elemental analysis						S_{DA}	$V_{micropores}$	Fe_{Bulk}	Fe_{XPS}	Fe_{XPS}/Fe_{Bulk} ratio
	C (%)	H (%)	N (%)	S (%)	Ash (%)	O (%)	(m^2/g)	(cm^3/g)	(wt. %)	(wt. %)	
GS	55.8	6.8	2.3	n.d.	3.5	31.6	0	0	-	-	-
GS-0	81.8	2.2	1.9	n.d.	9.4	4.7	405	0.14	-	-	-
GS-1	76.3	2.3	1.5	n.d.	8.2	11.7	440	0.16	-	-	-
GS-2	71.0	2.3	4.0	n.d.	8.1	14.6	376	0.14	-	-	-
GS-3	70.1	2.3	2.9	n.d.	7.3	17.4	506	0.19	-	-	-
Fe-GS-1	73.8	2.1	2.6	n.d.	12.0	9.5	416	0.15	2.8	11.0	3.9
Fe-GS-2	69.0	2.4	3.1	n.d.	10.9	14.6	348	0.12	4.7	7.6	1.8
Fe-GS-3	67.0	2.2	2.7	n.d.	9.6	18.5	483	0.17	3.9	12.8	3.3

n.d. not detected

Table 2. BPA, TOC and H_2O_2 conversion with Fe-GS-1, Fe-GS-2 and Fe-GS-3 catalysts after 4 h reaction time ($[BPA]_o$: 100 mg L^{-1}, $[H_2O_2]_o$: 530 mg L^{-1}, T: 50 °C, pH_o: 3).

Catalyst	BPA conversion (%)	TOC reduction (%)	H_2O_2 conversion (%)
Fe-GS-1	100	26	35
Fe-GS-2	10	0	3
Fe-GS-3	100	22	27

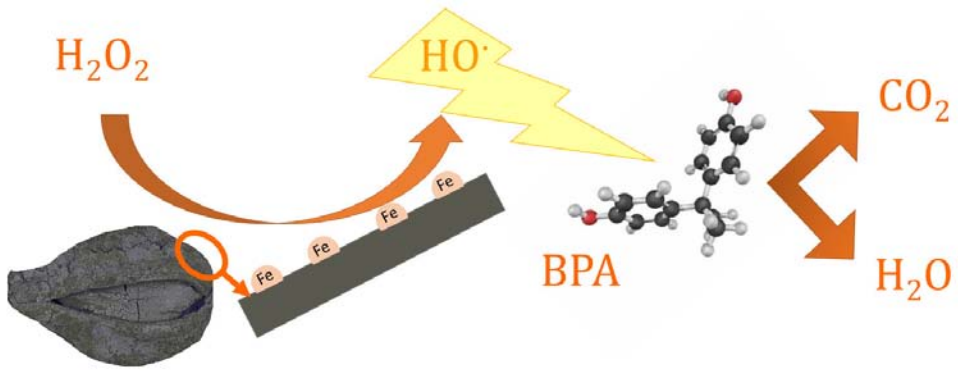

Highlights

- Fe catalyst were prepared on pyrolized and activated grape seeds support.
- Fe-GS-1 catalyst was highly active and stable upon CWPO of BPA.
- Complete removal of BPA and 60 % mineralization was reached at 80ºC.
- BPA CWPO enhanced the biodegradability and reduced the toxicity of the effluent.